

# Behavior Of Composite Girders Strengthened By CFRP Products

Prof. Dr. Nameer A. Alwash, Majid Adhab Jaber

**Abstract:** Composite structures are widely used in civil engineering projects. The present research consecrated to study the behavior of (steel-concrete) composite girders consisting from high strength concrete deck slab integrated with two steel I-beam by headed steel stud connectors. The present research implemented experimental and theoretical investigation. In the experimental investigation, five models were constructed as test samples. The test samples designed to be tested and failed in flexure. The dimensions of deck slab for each sample are (1000x2000x70mm: widthxlengthxthickness), while the dimensions of each I-beam are (142x2000mm: depthxlength). The test samples un-strengthened and strengthened externally by CFRP sheets with different manner and using and un-using CFRP bars instead of ordinary steel reinforcements. Theoretical investigation conducted by modeling the test samples numerically and analyzed using finite element method. The numerical models were carried out in three dimensions by software package (ANSYS 12.1, 2009). Verification of the numerical results was done by a comparison with experimental results. It is concluded that the strengthening of bottom face of concrete slab and bottom face of the bottom flanges of the steel beams by CFRP sheets increases the ultimate load values by (4%) but there is no considerable enhancement in the deflection and slip values. There is a slight structural advantage in case of using CFRP bars instead of ordinary steel bars reinforcements.

**Index Terms:** Steel-Concrete Composite Construction, Composite Girders, CFRP laminates, CFRP bars, Finite Element Analysis..

## 1 Introduction

The definition of composite construction or composite section is connecting different materials together in order to build a composite structural member with desirable properties of the materials. Composite girders can be constructed from concrete deck slab and steel I-beam connected together by steel headed studs, such construction was adopted in the present investigation. The main advantages of such construction are: (1) avoid high depth of girders and then excessive self-weight especially for the case of long span. (2) Increase the stiffness of the member by: a. resisting the tensile stresses by steel I-beam to avoid weak resistance of concrete in tension zone of the girders. b. resisting compressive stresses by concrete deck slab to avoid the problem of buckling of steel in compression zone of the girders. The performance of composite section is controlled by composite action. Composite action is the degree of the connection (or bond) between the concrete deck slab and steel I-beam. The degree of composite action is mainly affected by mechanical and geometrical properties of shear connectors. The degree of the composite action is ranging between case of zero bond when there is no shear connectors between the integrated material and case of full bond when there is enough number of shear connectors. In case of full bond, one can assume there will be no relative slip occurred between concrete slab and steel beam and the two components will act as one unit. Non-deformable connectors may cause excessive bearing stresses which may cause crushing in concrete, due that complete connection is not preferable in composite section<sup>[1,2,3]</sup>.

Shear connectors is used to resist longitudinal slip along the contact surface and consequently resist shear forces, in addition to that resist the vertical splitting forces which try to separate the composite materials. Fig.(1) shows some types of shear connectors. Stud headed shear connector is the most popular type of connecting device to be used in composite construction. Tee and channel connector resist shear forces in one direction only while the headed stud can resist shear forces similarly in any direction within the plane of slip surface. The headed stud connectors are more available, simple in welding, no obstruction reinforcements and not costly.

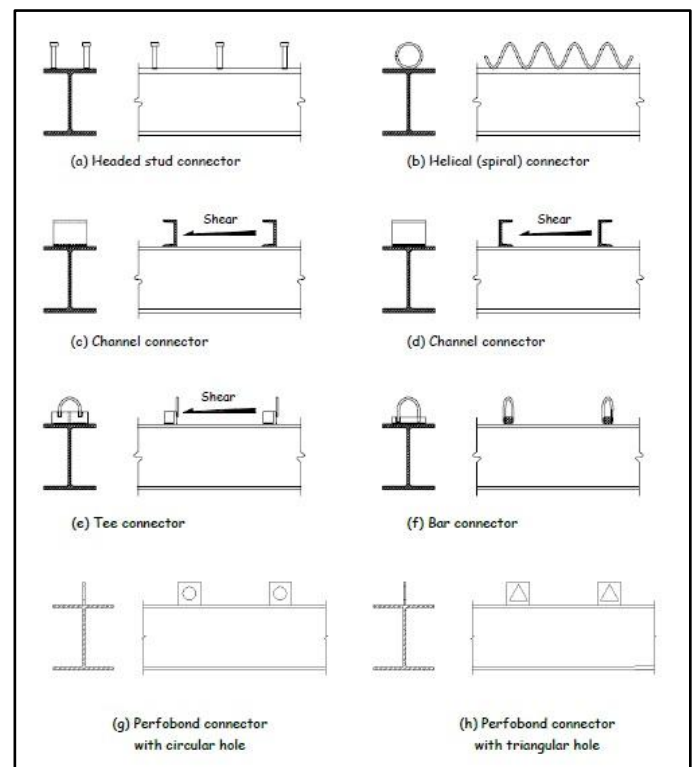


FIG.(1) Some Types of Shear Connectors<sup>[4,5,6,7]</sup>

- Dr. Nameer A. Alwash, Prof. College of Eng. University of Babylon-Iraq, Email: [namer\\_alwash@yahoo.com](mailto:namer_alwash@yahoo.com)
- Majid Adhab Jaber, Lecturer College of Eng. University of Kufa-Iraq, E-mail: [majidaj.alwaeli@uokufa.edu.iq](mailto:majidaj.alwaeli@uokufa.edu.iq)

**G. Foretet**, al. [8], in 2005, investigated the behavior of two-way reinforced concrete slab strengthening by CFRP strips bonded to the tensile face. Experimental investigation was conducted on RC two-way slabs strengthened with CFRP strips. A 2-D finite element for orthotropic composite plates was used to describe elastic behavior of RC slabs strengthened with CFRP strips.

**H. A. Jabir**[9] carried out, in 2006, a nonlinear three-dimensional finite element analysis to predict the load-deflection behavior of a composite girder consisted of a reinforced concrete slab and a steel beam with shear connectors under static and transient loads using the analysis system computer program (ANSYS 5.4).

**K. Bartha and H. Wu**[10], in 2006, carried out an experimental investigation by fabricating two composite steel girders consisted from high performance concrete and one four-span continuous composite steel bridge tested to failure and had been used to validate an proposed FEA models.

**M. S. Bachachi**[11], in 2007, carried out a theoretical investigation to predict load-deflection behavior of composite beams consisting of a reinforced concrete slab and a steel beam with shear connectors under static loads. The composite beams were modeled by using software package (ANSYS 9) as a nonlinear three dimensional finite element model. In 2010,

**F.A. Mikhail** et al. [12] studied the effect of pre-intermediate separation on the flexural behavior of strengthened steel-concrete composite beams by either adhesively bonded carbon fiber reinforced polymers (CFRP) sheet or welded/bonded steel plate. In 2011,

**E. L. Tana and B. Uy**[13] introduced a three dimensional finite element model to simulate composite steel-concrete beams subjected to combined flexure and torsion. The authors considered the influence of partial shear connection. The numerical model conducted using software (ABAQUS).

## 2 Samples Details

Experimental investigation implemented construction and testing five samples, each sample is consisting from concrete deck slab and two steel I-beams connected together by steel headed studs. Fig.(2) shows the dimensions of the test sample. Dimensions of concrete deck slab are (1000×2000×70mm:width×length×thickness),and reinforced with double layer of mesh wire of size (5.6 mm) diameter and opening size of (150 mm).

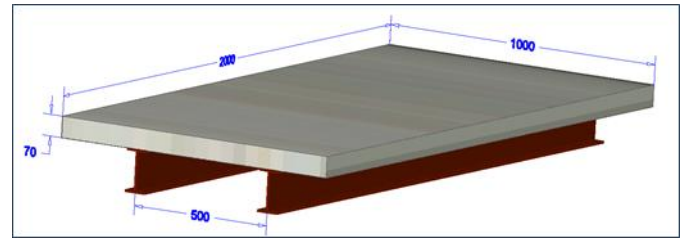


**FIG.(2)** Composite Steel-Concrete Sample (Dimensions in millimeter)

Ordinary reinforcement of one of the samples replaced by CFRP bars size (6mm) with two layers and spacing (200mm c/c) in both directions. The dimensions of steel I-beam are (142×2000mm: depth×length). Headed steel studs (shear connectors) were welded to the top flange of each I-beam. The diameter of used shear connectors is (9.8 mm) and overall length of (40mm).Fig.(3) shows the typical cross section of the tested samples in the investigation

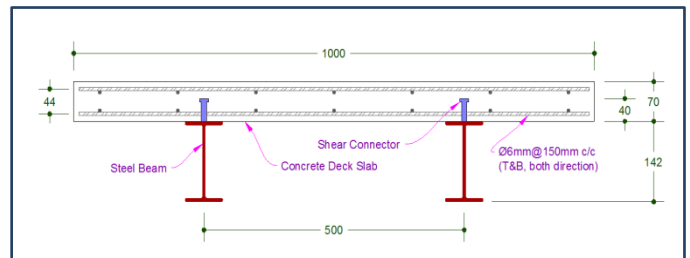


**FIG.(3)** Cross Section of a Typical Sample (Dimensions in millimeter)

Each test sample contains (38) shear connectors, (19) shear connectors for each I-steel beam. The shear connectors were uniformly distributed along the longitudinal axis of each I-steel beam by spacing of (100 mm) center to center of headed stud shear connector. The test samples are named as (BG1, control sample), (BG6), (BG7), (BG8), and (BG9). All the samples are loaded monotonically by two line loads, applied at distance of (320 mm) from the mid-span for each line. The test samples were simply supported during the test. Fig.(4) shows distribution and number of shear connectors for the test samples.

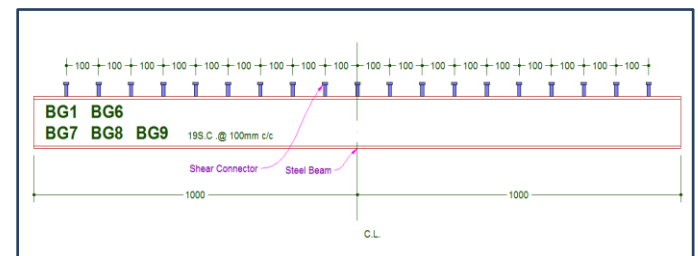
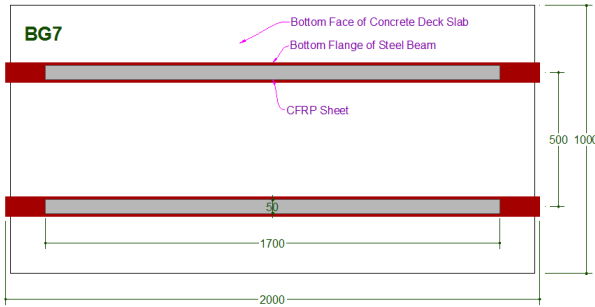


**FIG.(4)** Distribution of Shear Connectors(Dimensions in millimeter)

Pattern of fixing CFRP sheets for the test samples (BG7,



BG8, and BG9) shown in Fig.(5)

FIG.(5) Distribution of CFRP Sheets(Dimensions in millimeter)

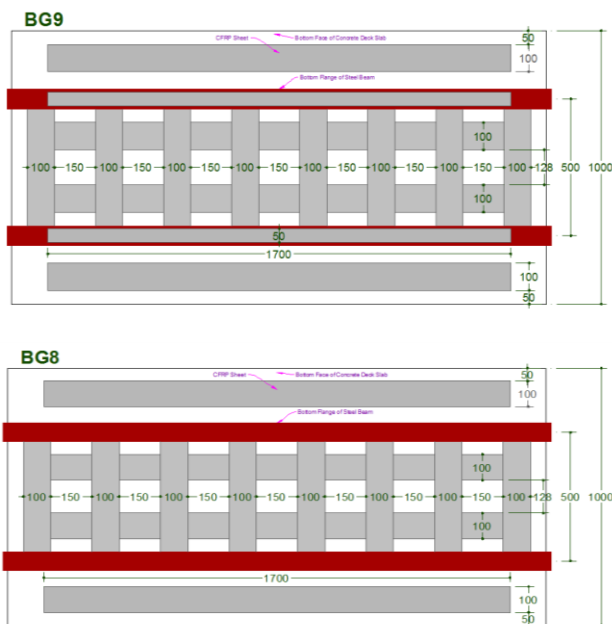


FIG.(5) Continued

(BG1) is the control sample which constructed without any strengthening by CFRP products. The concrete deck for (BG6) was reinforced by CFRP bars.

### 3 Properties of Materials

#### 3.1 Steel Beam

Steel beams of I-section shape were used in constructions the tested samples. The type of steel beam is (European IPE 140). The material of the steel beam was tested according to (ASTM A370). Table (1) shows the properties of the steel beam.

Table (1) Properties of Steel Beam

Sectional Area (mm <sup>2</sup> )	I <sub>x</sub> (mm <sup>4</sup> )	Steel Grade	Yielding Stress σ <sub>y</sub> (MPa)	Tensile Strength σ <sub>u</sub> (MPa)
1645	5.28 x10 <sup>6</sup>	ST 37	344	494

Depth	Flange Width	Flange Thickness	Web Thickness	Radius of Curvature	Unit Weight
142 mm	72 mm	6.5 mm	5.5 mm	7 mm	13 kg/m

#### 3.2 Headed Steel Stud Shear Connector

The stud shear connectors were used after cutting the threaded part from the original bolts of type (M.H 8.8). Overall length (40 mm) and diameter (9.8 mm) and head diameter (17 mm) and height of head (6.3 mm) were used in construction of test samples. The yielding stress for studs is (σ<sub>y</sub>=240MPa) and tensile strength (σ<sub>u</sub>=1010MPa).

#### 3.3 Ordinary Steel Reinforcement of Concrete

The type of steel reinforcement used in this study was (MD 25), two layers of mesh steel wire reinforcement (BRC) of deformed bars with diameter (5.6 mm) and spacing (150 mm c/c) in both directions. The area of steel given by such reinforcement is (170 mm<sup>2</sup>/m) for one layer. The yielding stress is (σ<sub>y</sub>=462MPa) and tensile strength (σ<sub>u</sub>=507MPa).

#### 3.4CFRP Products

Two types of CFRP products were used in the present investigation; one of them was CFRP sheets manufactured by (Sika) company. The product named (SikaWrap-230 C). While the other one was CFRP bars manufactured by (Aslan) company, named (Aslan 201). CFRP sheet (SikaWrap-230 C) is a unidirectional woven carbon fabric for the dry application process, some of properties delivered with the product shown in Table (2).CFRP sheet (SikaWrap-230 C) was used with special epoxy which mentioned in Table (2) named as (Sikadur-330).

Table (2) Properties of CFRP Sheets

Product Data	
Fiber Type	Mid strength carbon fibers.
Fabric Construction	Fiber orientation: 0o (uniderctional).
	Wrap: black carbon fibers (99% of total areal weight).
	Weft: white thermoplastic heat-set fibers (1% of total areal weight).
Packaging	Roll of width (300 mm).
Technical Data	
Areal Weight	230 g/m <sup>2</sup>
Fabric Design Thickness	0.131 mm
Fiber Density	1.76 g/cm <sup>3</sup>
Mechanical / Physical Properties	
Dry Fiber Properties	Tensile strength: 4300 MPa
	Tensile E-Modulus: 238 GPa
	Elongation at break: 1.8 %
Laminate Properties	Laminate thickness: 1 mm/layer (impregnated with Sikadur-330).
	Ultimate load: 350 kN/m width per layer (at typical laminate thickness of 1 mm).
	Tensile E-modulus:

	28 GPa (based on typical laminate thickness of 1 mm)
System Information	
System Structure	The system configuration must be fully complied with and may be not be changed. Concrete primer: Sikadur-330 Impregnating / laminating resin: Sikadur-330 Structural strengthening fabric – SikaWrap-230 C.

CFRP bars were used as embedded reinforcement inside the concrete for one of the five test samples. CFRP bars (Aslan 201) were tested by the processed company according to (ASTM D7205) and the results related to the mechanical and physical properties are shown in Table (3).

**Table (3)** Properties of CFRP Bars

TEST	RESULT	SPECIFICATION
(ASTM D7205)		
Nominal Diameter (mm)	6	---
Cross Sectional Area (mm <sup>2</sup> )	31.67	---
Bar Length (m)	3	---
Tensile Strength (MPa)	2704	≥ 2068
Modulus of Elasticity (GPa)	163	≥ 124

### 3.5 Concrete

The materials (fine aggregate, coarse aggregate, cement, and water) used in preparing the concrete was tested according to the standards specifications. Mixing of concrete was carried out using electrical tilting drum mixer.

## 4 Experimental Results

The obtained results from the experimental testing of the present study are:

- Deflections at:
  - Central point of the sample which lies at bottom face of the concrete slab. The symbol of the deflection at this point is (DCC).
  - Mid-span point of one of the steel beams which lies at bottom face of bottom flange of the steel beam. The symbol used for this point is (DCS).
  - Points beneath the two line loads at bottom face of bottom flange of the steel beam. The symbols used for these points are (D1) and (D2).
- Slip at ends between concrete slab and one of the steel beams. The symbols of these slips are (S1) and (S2).

All of the for-mentioned results were recorded at each stage of loading. The value of load was obtained from analog reader of the test machine. The experimental data were obtained by using dial gauges for deflection and slip, demec discs and extensometer for normal strain. Table (4) shows the ultimate load recorded for each sample and the load of

first crack formed in concrete slab and the ratio between the two loads. In addition to that, values of compressive strength of the concrete of each sample are listed. Sample (BG1) is the control sample, it was failed under ultimate load of ( $P_u=405$  KN). Sample (BG6) was reinforced with CFRP bars embedded (instead of ordinary steel reinforcements) in concrete slab. This type of reinforcing causes an increase in the capacity of ultimate load by a ratio of (5%). The ultimate load was increased from (405 kN) to (425 kN) only. The test samples (BG7, BG8 and BG9) was strengthened with CFRP sheets and there is an increase of ultimate load from (405 kN) to (435, 422 and 442 kN) for (BG7, BG8 and BG9) consequently. The reasons of this increase in ultimate capacity are strengthening of the extreme fibers in tension face of concrete slab section for (BG7) and at steel beams for (BG8) and at both of them for (BG9). The predicted increasing ratios for ultimate capacity are (7%, 4% and 9%) for samples (BG7, BG8 and BG9) consequently.

**Table (4)** Ultimate Load and First Crack Load

Sam ple	First Crac k Load $P_{cr}$ (k N)	Ultimat e Load $P_u$ (kN)	$P_{cr}/$ $P_u$ (%)	Compressi ve Strength ( $f_{cu}$ )	Notes (considered parameter)	
BG1	185	405	46	55	Control Beam	
BG6	135	425	32	67	CFRP Concrete Reinforcement	
BG7	135	435	31	68	Strengthe n-ing with CFRP Sheets	
BG8	185	422	44	69		Steel and Con cret e
BG9	135	442	31	66		Steel and Con cret e

The compressive strength for the samples (BG6, BG7, BG8, and BG9) is higher than that for the control sample (BG1). This cause an increase in the ultimate load, for this reason, modified numerical models with compressive strength (55 MPa) was carried out. The modified numerical models for these samples show that the ultimate load for (BG6=437kN), (BG7=446kN), (BG8=428kN), and (BG9=454kN). Fig.(6) to Fig.(10) shows the state and the crack pattern of samples after test.



**FIG.(6)** Crack Patterns at Failure for BG1-Control Sample



**FIG.(8)** Crack Patterns at Failure for BG7



**FIG.(7)** Crack Patterns at Failure for BG6



**FIG.(9)** Crack Patterns at Failure for BG8



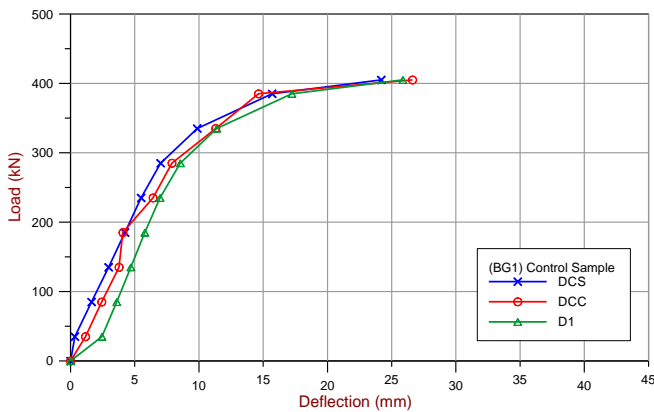
**FIG.(10)** Crack Patterns at Failure for BG9

Table (5) shows the recorded data of deflection for all the tested samples at the ultimate loads.

**Table (5) Maximum Deflections**

Sample		BG1	BG6	BG7	BG8	BG9
Ultimate Load $P_u$ (kN)		405	425	435	422	442
Deflection (mm)	DCS	24.1 9	39.1 9	31.3 6	34.5 2	32.1 2
	DCC	26.6 2	39.0 3	27.3 0	34.2 8	33.2 5
	D1	25.8 7	31.3 8	27.4 7	29.2 4	27.5 6
	D2	--	33.9 9	24.0 9	32.7 9	29.8 4

The response of each test sample is presented through load-deflection curves shown in Fig.(11) to Fig.(15).



**FIG.(11) Load-Deflection Curve (BG1)**

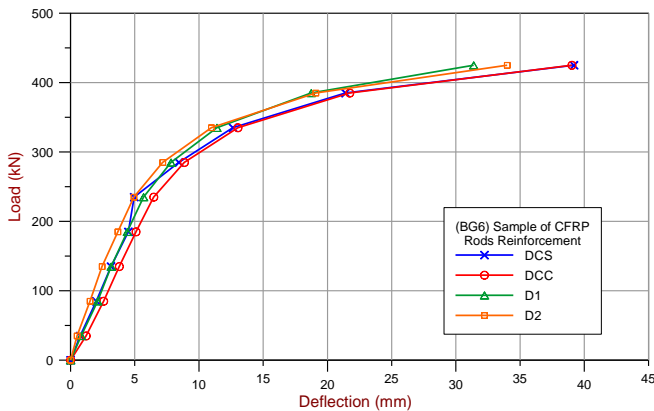


**FIG.(12) Load-Deflection Curve (BG6)**

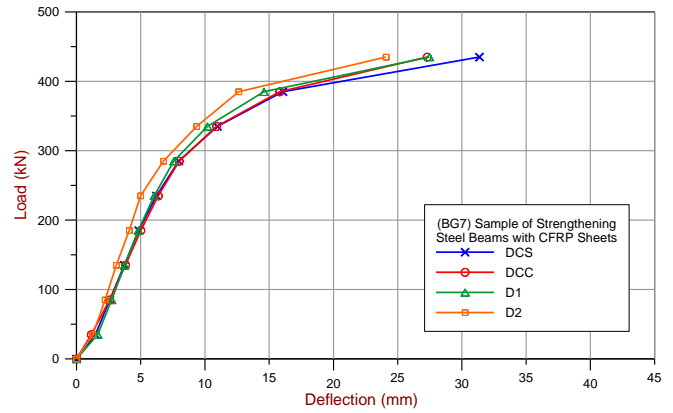


**FIG.(13) Load-Deflection Curve (BG7)**

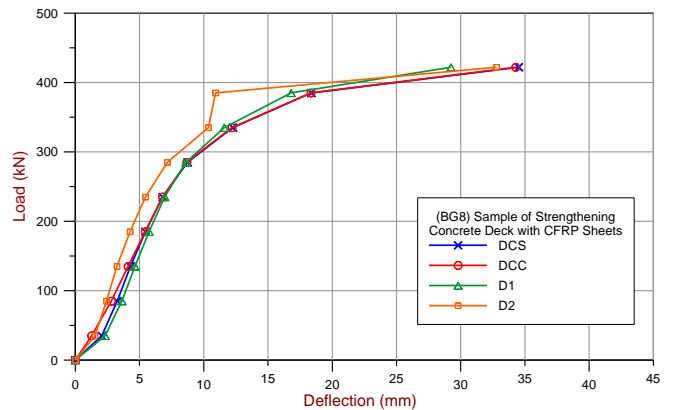


**FIG.(14) Load-Deflection Curve (BG8)**

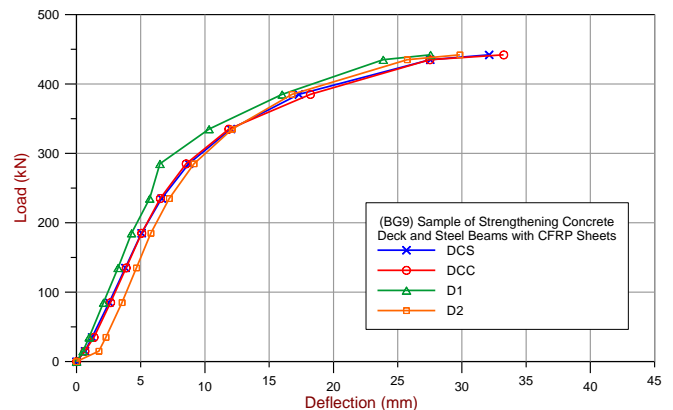


**FIG.(15) Load-Deflection Curve (BG9)**

Reviewing the previous curves and tables of deflection indicates the maximum deflection always occurs at mid-span either in concrete deck or in steel beams. The difference in deflection between concrete deck and steel beam may be due to flexural effect in transverse direction (short direction) of the concrete deck slab. Fig.(16) and Fig.(17) show a comparison between the control sample (BG1) and the other test samples for a deflection of the steel beams at mid-span point (DCS) which is lowest point in the test samples.

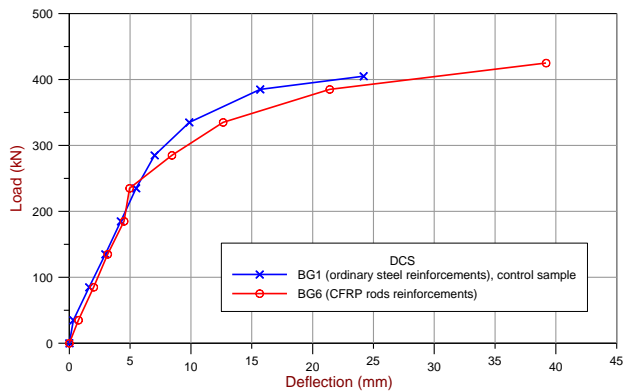


**FIG.(16) Effect of CFRP Bars on Load-Deflection Response (deflection at mid-span point of steel beam)**

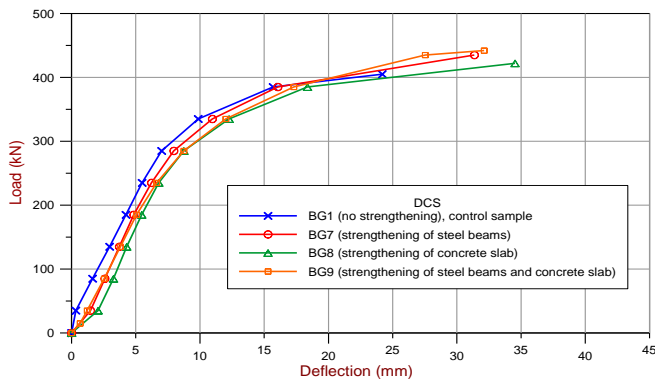


**FIG.(17) Effect of Strengthening Concrete Deck by CFRP Sheets on Load-Deflection Response (deflection at mid-span point of steel beam)**

Reinforcing concrete deck slab by CFRP bars instead of steel reinforcement (BG6) did not produce an obvious advantage in sample capacity. However, deflection of sample (BG6) was greater than that for control sample (BG1). Maximum deflection corresponding to the ultimate load was increased by a percentage of (62%) while increasing of corresponding ultimate load was only by a percentage of (5%). Besides that, there is an increasing in the slope of load-deflection curve at advanced loading increments. That is due to the contribution of the high stiffness of CFRP bars after cracking of the concrete deck and yielding of the steel beams. Strengthening with CFRP sheets indicates that the strengthening of steel beams (BG7 and BG9) provide a greater increasing percentage of ultimate load with a less increasing percentage in maximum corresponding deflection. While strengthening of concrete deck (BG8) provide a smaller increasing percentage of ultimate load with a greater increasing percentage in maximum corresponding deflection. In addition to that, there is an obvious increasing in the stiffness of the samples (BG7, BG8, and BG9) in the second half of loading process. This is may be caused by the contribution of high stiffness of CFRP sheet. End slips at the ends of one of the steel beams were recorded for each load increment. End slip readings are denoted as (S1) and (S2). Fig.(18) shows the load versus average slip of (S1 and S2) for all tested samples. The comparison of the end slip results for the tested samples (BG7, BG8, and BG9) shows

that the end slip results of samples are less than that for control sample (BG1). This means that the CFRP sheets enhanced the slip behavior. Reinforcement of concrete deck with CFRP bars did not improve the slip behavior of the girder.

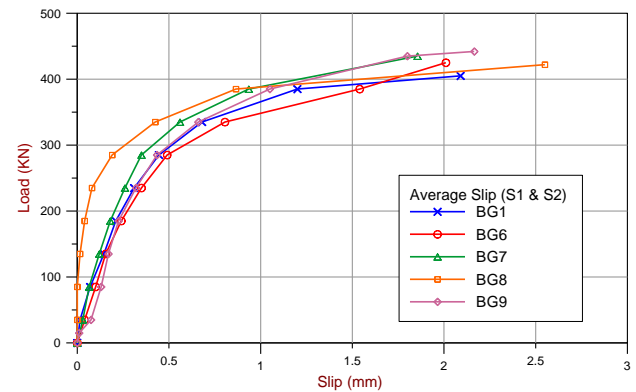


**FIG.(18) Load-Slip (ave. slip of S1 & S2) Curve of Test Samples**

## 5 Finite Element Modeling

Finite element analysis, as used in structural engineering, determines the overall behavior of a structure by dividing it into a number of single elements, each of which has well-defined mechanical and physical properties. Modeling of the constitutive materials properties is an important aspect of any finite element analysis. The constitutive model should be correctly describing the behavior of the material under uniaxial and multi-axial states of loading. Finite Element modeling and analysis were carried out to simulate the behavior of the five tested composite steel-concrete girders from linear through nonlinear response and up to failure, using the (ANSYS 12.1) program [14]. The choice of the proper element type is very important in the finite element analysis. The chosen element type depends upon the geometry of the structure and the number of independent space coordinates necessary to describe the problem. Composite members are made of different materials i.e. steel, concrete, shear connectors and reinforcing bars, which are brought together to constitute a composite system. Each component of composite member should be modeled by the proper element type and then should be provide each type of element by the properties according to the material of that component. In the present study, three dimensional model was used to analyze composite girders consisting from concrete deck slab and two I-steel beams integrated by steel studs shear connectors. The concrete slab was divided in its length, width, and depth into brick element (SOLID65). Element type (SHELL43) (or 4-node plastic small strain shell) was used to model steel I-beam. Reinforcement of concrete and stud connectors were modeled by element type (LINK8). Element (COMBIN39) was used, in this study, to simulate the behavior of the shear connectors in resisting the tangential forces between the concrete slab and the I-steel beams. The contact between concrete slab and steel beams produce normal forces and tangential forces acting on the plane of contact. This action modeled by using 3-D point-to-point contact element called (CONTAC52). Studying the effect of shear connectors number and



distribution faces a difficulty in simulation the connectivity between stud's elements with concrete and steel beams elements. If the bond between concrete slab and steel beams is fully bond (which can be achieved by using excessive number of studs) this difficulty will be solved by connecting directly the neighboring concrete elements and steel beams elements through concerted nodes. Thus, a need for using more types of elements is appear to represent the bond action between concrete slab and steel beams. Fig.(19) shows the overall finite element meshing of the test samples.

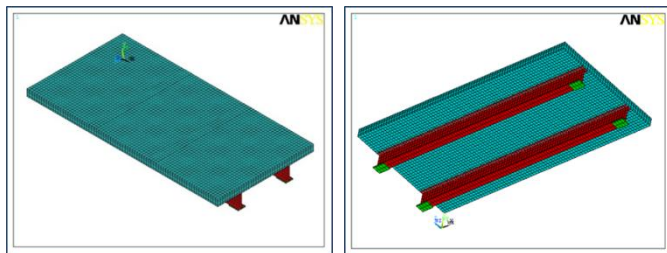


FIG.(19) Geometry of the Numerical Model

**6 Finite Element Analysis Results**

The numerical results of ultimate loads, vertical deflection, and horizontal slip are concerned to compare them with those of experimental work. This comparison was conducted to verify the numerical model. Table (6-a) shows a comparison between experimental and numerical ultimate loads for the study samples. Table (6-b) shows a comparison between numerical samples (with different compressive strength of concrete slab as the experimental samples) and modified numerical samples (with equal compressive strength 55 MPa as the control sample). In general, the ultimate loads which predicted by the numerical analyses are rather greater than those of experimental testing.

**Table (6-a) Comparison of Load and Deflection at Service and Ultimate Stages for the Tested Samples**

Sample		BG 1	BG 6	BG 7	BG 8	BG 9
Service Load 65% of Ultimate Load	Exp.	263	276	283	274	287
	Num.	278	290	297	286	301
	Difference %	5.4	5.1	5.2	4.3	4.7
Deflection (DCS) at Service Load (mm)	Exp.	6.35	7.82	7.88	8.32	8.89
	Num.	6.66	6.89	7.00	6.69	7.13
	Difference %	4.8	-	-	-	-
Ultimate Load P <sub>u</sub> (kN)	Exp.	405	425	435	422	442
	Num.	427	447	458	440	463
Deflection (DCS) at Ultimate Load (mm)	Exp.	24.1	39.1	31.3	34.5	32.1
	Num.	25.7	35.6	29.5	28.5	31.1
	Difference %	6.4	-9.1	-5.9	-17.4	-3.1

**Table (6-b) Comparison of Load and Deflection at Service and Ultimate Stages for the Numerical Samples and Modified Numerical Samples**

Sample		BG 1	BG 6	BG 7	BG 8	BG 9
Service Load 65% of Ultimate Load	Mod. Num.	278	284	290	278	295
	Num.	278	290	297	286	301
	Difference %	0	2.07	2.36	2.80	1.99
Deflection (DCS) at Service Load (mm)	Mod. Num.	6.66	6.72	6.79	6.49	6.99
	Num.	6.66	6.89	7.00	6.69	7.13
	Difference %	0	2.47	3.00	2.99	1.96
Ultimate Load P <sub>u</sub> (kN)	Mod. Num.	427	437	446	428	454
	Num.	427	447	458	440	463
Deflection (DCS) at Ultimate Load (mm)	Mod. Num.	25.7	29.2	25.0	24.2	24.5
	Num.	25.7	35.6	29.5	28.5	31.1
	Difference %	0	18.0	14.9	15.0	21.0

The percentage of difference between experimental tests and numerical analyses for the ultimate loads is between (4.3-5.4) % for all the samples as shown in Table (6-a). The deflection in numerical models is in general smaller than that in experimental samples and the percentages of variation are between (3.1-17.4)% at the ultimate load and (11.2-19.8)% at the service load (65% of ultimate load). The exception is that, numerical deflection of sample (BG1) is little greater than that in the experimental sample. The percentage variation for sample (BG1) is (6.4%) at the ultimate load and (4.8%) at service load. The percentage of variation in deflection for sample (BG1) is very small, it is almost equal zero. Hence, In general the numerical models are stiffer. The following figures (20-34) show a comparison between experimental and numerical results for deflection and slip.

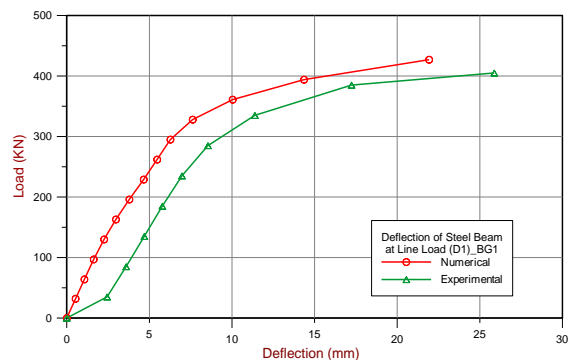
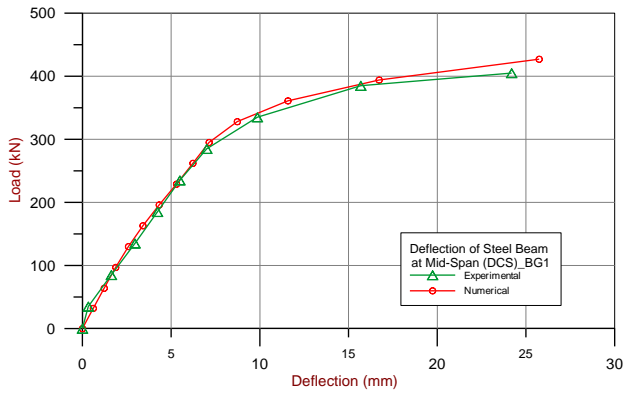
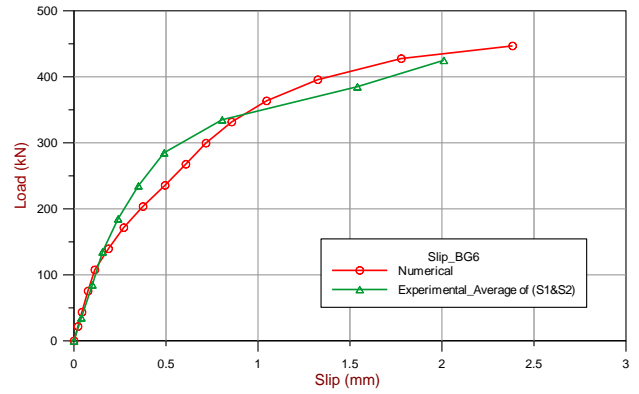


FIG.(20) Experimental and Numerical Load Deflection (D1) Curves of Sample(BG1)





**FIG.(21)** Experimental and Numerical Load Deflection (DCS) Curves of Sample(BG1)



**FIG.(24)** Experimental and Numerical Load Deflection (DCS) Curves of Sample(BG6)

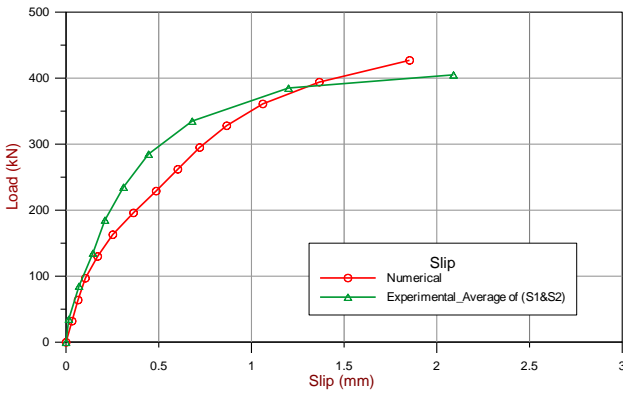


**FIG.(22)** Experimental and Numerical Load Slip Curves of Sample(BG1)

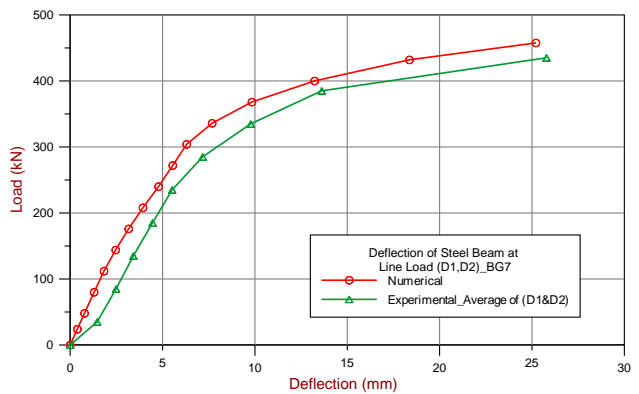


**FIG.(25)** Experimental and Numerical Load Slip Curves of Sample(BG6)

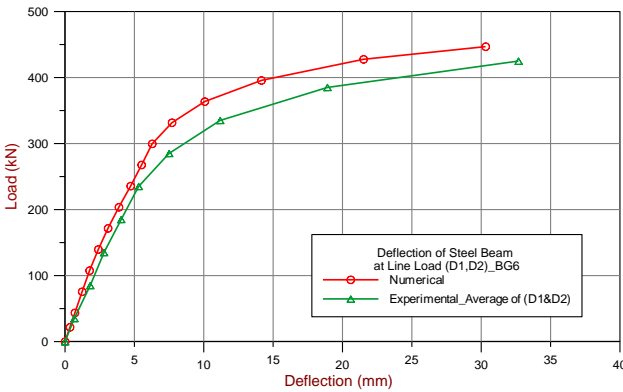


**FIG.(23)** Experimental and Numerical Load Deflection (D1 and D2) Curves of Sample(BG6)

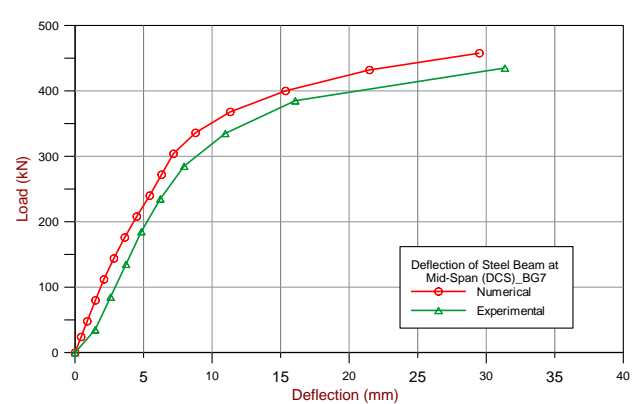


**FIG.(26)** Experimental and Numerical Load Deflection (D1 and D2) Curves of Sample(BG7)

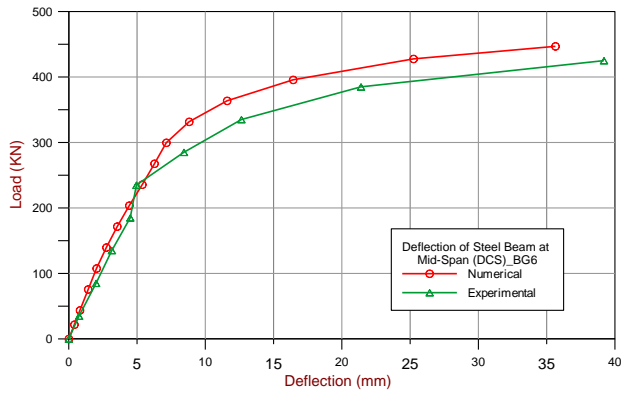


**FIG.(27)** Experimental and Numerical Load Deflection (DCS) Curves of Sample(BG7)

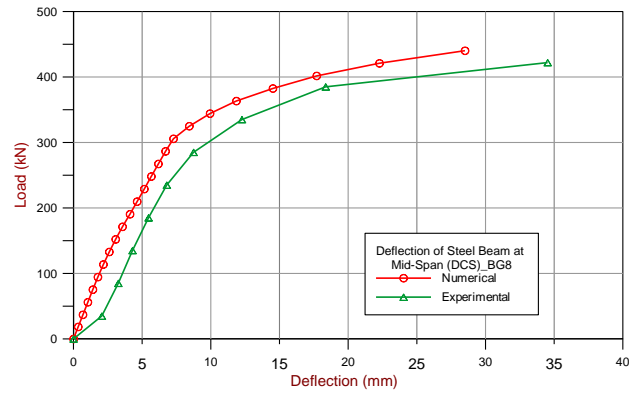


**FIG.(30)** Experimental and Numerical Load Deflection (DCS) Curves of Sample(BG8)

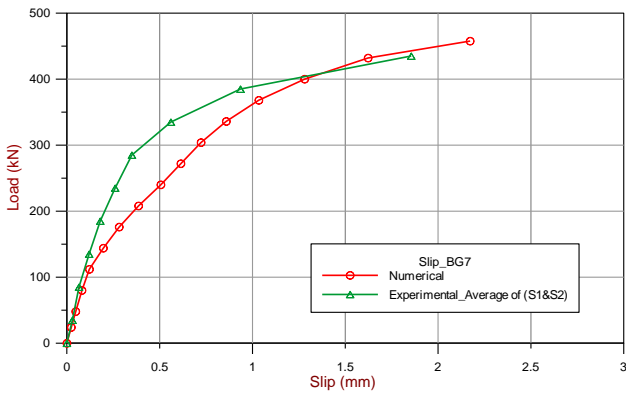


**FIG.(28)** Experimental and Numerical Load Slip Curves of Sample(BG7)

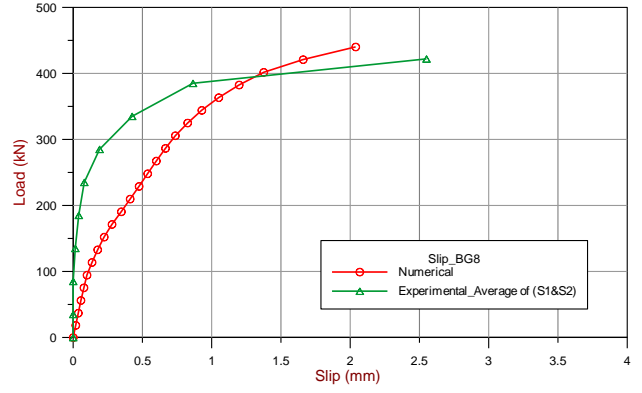


**FIG.(31)** Experimental and Numerical Load Slip Curves of Sample(BG8)

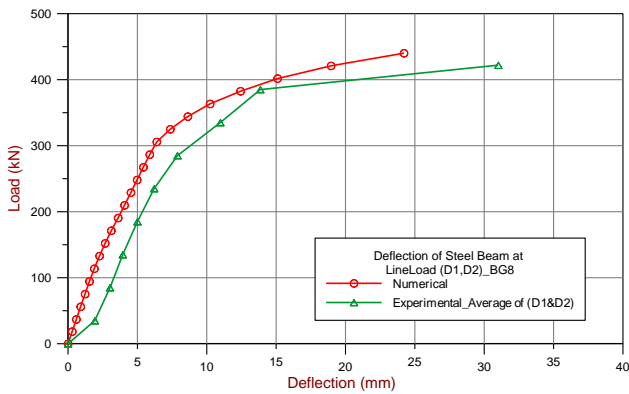


**FIG.(29)** Experimental and Numerical Load Deflection (D1 and D2) Curves of Sample(BG8)

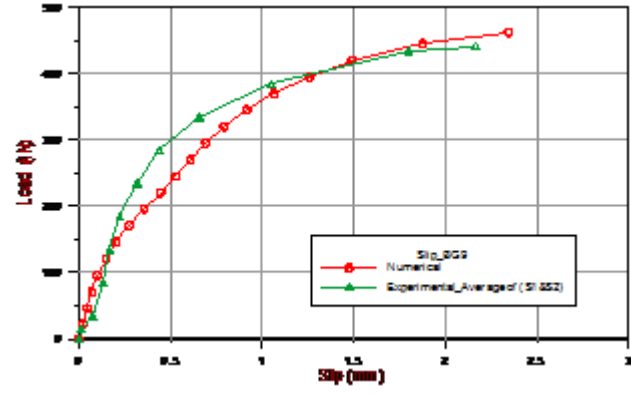


**FIG.(32)** Experimental and Numerical Load Deflection (D1 and D2) Curves of Sample(BG9)

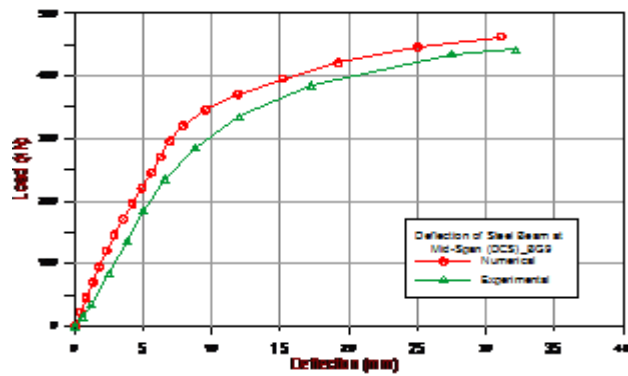


**FIG.(33)** Experimental and Numerical Load Deflection (DCS) Curves of Sample(BG9)

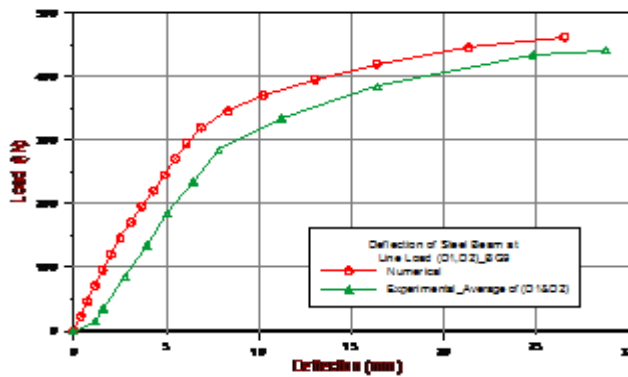


**FIG.(34)** Experimental and Numerical Load Slip Curves of Sample(BG9)

The comparison of the results shows in general that the numerical models are stiffer, and the numerical analyses give a smaller result for the deflection and greater for ultimate load. The results of slip show that there is a deviation in results in the middle third of loading stages and there is a good convergence at approximately the last third of loading stages. This may be caused by the following: 1. The concrete of experimental samples is not perfectly homogeneous as assumed in the numerical models. 2. Micro cracks which may have happened in concrete due to shrinkage reduce the stiffness in some degree. 3. Cutting and welding process of the stud connectors produce initial stresses in the studs and the steel beam. 4. Perfect bond between concrete and steel or CFRP reinforcements is assumed in the finite element analyses, but in the experimental samples this bond is not perfect and there is a slip which causes a loss in composite action.

## 6 Conclusions

The general behavior during test process is similar for all tested samples. The first cracks are formed at about (31-44) % of ultimate load for tested samples. The general trend of the ultimate load values is to increase with strengthening by CFRP sheets. Strengthening bottom face of concrete slab and bottom face of the bottom flanges of the steel beams by CFRP sheets slightly increases the ultimate load values by about (4%) but there is no considerable enhancement in the deflection and slip values. Considering the high cost and slight effect of the CFRP bars, leads to

conclude that there is no structural advantage of using CFRP bars instead of ordinary reinforcement of concrete slab. However, as known, it is more durable than steel reinforcement. The adopted finite element modeling in general overestimates the ultimate load in comparison with the experimental results. The deviation is only in the range from (4.3%) to (5.4%).

## References

- [1] H. W. Al-Thebhawi "Nonlinear Finite Element Analysis of Composite Steel-Concrete Beams". Ph.D. Thesis, University of Technology, 2005.
- [2] S. S. Kadhim "Finite Element Analysis of Composite Concrete-Steel Arches up To Failure". M.Sc. Thesis, University of Tikrit, 2007.
- [3] A. Y. Zainul-Abideen "Experimental and Theoretical Investigation of Composite Steel-Concrete Arches". Ph.D. Thesis, University of Technology, 2010.
- [4] R. P. Johnson "Composite Structures of Steel and Concrete". Volume 1, 1994.
- [5] D. A. Nethercot "Composite Construction", 2004.
- [6] Cosenza, E. and Zandonini, R. "Composite construction". Structural Engineering Handbook, Ed. Chen Wai-Fah, Boca Raton: CRC Press LLC, 1999.
- [7] S. Y. Al-Darzi and M. A. Al-Juboory "Investigation of Steel-Concrete Composite Beams with Different Types of Shear Connectors". Tikrit Journal of Engineering Sciences/Vol.20/No.3/March 2013, (32-40).
- [8] G. Foret et al. "Numerical and Experimental Analysis of Two-Way Slabs Strengthened with CFRP Strips". Journal of Engineering Structures 27, 2005.
- [9] H. A. Jabir "Finite Element Analysis of Composite Concrete-Steel Girders under Static and Transient Loading". M.Sc. Thesis, University of Technology, 2006.
- [10] K. Barth, H. Wu "Efficient Nonlinear Finite Element Modeling of Slab on Steel Stringer Bridges". Finite Element Analysis and Design 42, 2006.
- [11] M. S. Bachachi "Nonlinear Analysis of Composite Concrete-Steel Beams under Bending Loads by Finite Element Method". M.Sc. Thesis, University of Technology, 2007.
- [12] Mikhail et al. "Flexural Behavior of Strengthened Steel-Concrete Composite Beams by Various Plating Methods". Journal of Constructional Steel Research 66, 2010.
- [13] E. L. Tan, B. Uy "Nonlinear Analysis of Composite Beams Subjected to Combined Flexure and Torsion". Journal of Constructional Steel Research 67, 2011.
- [14] ANSYS "ANSYS Help". Release 12.1, USA, 2009.